2016

# Homocysteine and CSRP-3 protein in migrating neural crest cells: A quantitative and qualitative confocal microscopy study

Allysan R. White
*University of Northern Iowa*

# HOMOCYSTEINE AND CSRP-3 PROTEIN IN MIGRATING NEURAL CREST CELLS – A QUANTITATIVE AND QUALITATIVE CONFOCAL MICROSCOPY STUDY

An Abstract of a Thesis

Submitted

in Partial Fulfillment

of the Requirements for the Degree

Master of Science

Allysan R White

University of Northern Iowa

December 2016

# ABSTRACT

Congenital heart defects are one of the leading causes of infant death. High maternal blood serum levels of the amino acid homocysteine and the frequency of heart defects are correlated, but the immediate cause is unknown. During early embryonic development, a distinctive population of cells arises dorsally as the neural tube closes, forming the brain and spinal cord. These are the neural crest cells, which play a crucial role in the development of the nervous system, head skeletal, certain endocrine and connective tissues, and, notably, the heart's outflow region. These migratory cells will follow specific pathways and respond to signals encountered in order to further differentiate and arrive at their correct destinations. There is evidence that neural crest cells may be affected in their migration by abnormally high levels of homocysteine. Any failure of cells to migrate efficiently with regard to timing and direction might cause malformations in the developing embryo.

A microarray study performed by Rosenquist et al. (2007) revealed that a gene known as CSRP-3, (an acronym for cysteine and glycine rich protein 3) which codes for a member of the LIM (an acronym for the proteins involved: Lin 11, Isl-1, and Mec-3) domain protein group, is over-expressed in neural crest cells exposed to homocysteine. CSRP-3 protein is a nuclear transcription factor but is also involved in cytoskeletal mediation of cell adhesion and migration. CSRP-3 interacts with scaffolding proteins in order to carry out mitotic functions and cytoskeletal specialization for development. This gene's mRNA was found to be upregulated 177-fold in the presence of homocysteine.

I hypothesized that if homocysteine does up-regulate this gene in migrating neural crest cells, it would be detectable by immunostaining using a specific antibody, and could be quantitated, localized and compared with control embryos to provide new information. Neural crest cells, and possibly other cells over-expressing CSRP-3, would show higher intensity of immunofluorescence signal. After injecting homocysteine or saline only (control) into the amnion of stage 10-12 chick embryos and allowing further development, I localized and measured CSRP-3 fluorescence in four regions known to receive migrating neural crest cells: 1) the cardiac pathway region, the brain meninges of the myelencephalon and diencehpalon, 2) the paraxial mesenchyme lateral to the neural tube, 3) the periocular mesenchyme, and 4) the pharynx region. Using confocal microscopy, sectioned and whole mount embryos were examined after undergoing double immunolabeling using an antibody to CSRP-3 protein and an antibody that recognizes neural crest cells. Expressing cells were measured to yield a corrected ratio. Cells identified in the areas of interest were all found to show significantly brighter fluorescence compared to cells in control embryos, supporting and expanding the findings of Rosenquist et al (2007), and providing additional evidence for this mechanism of action of homocysteine.

# HOMOCYSTEINE AND CSRP-3 PROTIEN IN MIGRATING NEURAL CREST CELLS – A QUANTITATIVE AND QUALITATIVE CONFOCAL MICROSCOPY STUDY

A Thesis

Submitted

In Partial Fulfillment

Of the Requirements for the Degree

Master of Science

Allysan R White

University of Northern Iowa

December 2016

This Study by: Allysan R White

Entitled: Homocysteine and CSRP-3 Protein in Migrating Neural Crest Cells – A Quantitative and Qualitative Confocal Microscopy Study

has been approved as meeting the thesis requirement for the

Degree of Master of Science

| | |
|---|---|
| _____ | _____ |
| Date | Dr. Darrell Wiens, Chair, Thesis Committee |
| _____ | _____ |
| Date | Dr. Nilda Rodriguez, Thesis Committee Member |
| _____ | _____ |
| Date | Dr. Carl Thurman, Thesis Committee Member |
| _____ | _____ |
| Date | Dr. Kavita Dhanwada, Dean, Graduate College |

# ACKOWLEDGMENTS

This work would not have been possible without the University of Northern Iowa Biology Department and Dr. Darrell Wiens. Also my parents, Rich and Donna, and my patient and understanding fiancé, Brett.

To you all, Thank you.

TABLE OF CONTENTS

PAGE

# LIST OF FIGURES

FIGURE PAGE

# LIST OF TABLES

TABLE PAGE

# CHAPTER 1

# INTRODUCTION AND LITERATURE REVIEW

## The Early Embryo

The development of the embryo begins with the oocyte, as it differentiates, organizes, and grows in the long and arduous process of the hormone-mediated oogenesis. Then, at fertilization, fusion of the egg and sperm cell membranes occurs and the sperm's genetic material is added. At this time the egg is activated for development. Immediately following is cleavage, a rapid cellular division event resulting in the vast amounts of egg cytoplasm dividing into smaller cells called blastomeres. The blastomeres then undergo gastrulation, a process of massive rearrangement and migration that yields three germ layers. Cell proliferation slows but continues. Gastrulation begins with the formation of a two layered blastoderm rearranging to create a hollow structure: the outermost epiblast, the middle blastocoel, and the inner hypoblast. Three germ layers will arise as cell migration occurs through the blastocoel from the epiblast when given a signal from the hypoblast cells (summarized by Gilbert 2010). Gastrulation is identified by the formation of the primitive streak, where invagination of the mesoderm and endoderm germ layers occurs, leaving behind an outer germ layer called the ectoderm. The cell populations migrating through these areas are consistently changing based on cellular germ layer as well as migration signals. Hensen's node is a structure located at the anterior tip of the primitive streak that cells migrate through and then anteriorly form the notochord, prechordal plate, and medial region flanking the notochord and immediately segmenting into somites, resulting in the body axis of the chick. These

structures, that will eventually form the brain and spinal cord, will all appear by 24 hours of development (Hamburger and Hamilton (HH) stage 8) (Vasiev et al 2010; Hamburger and Hamilton 1951).

## Neural Crest Cells

Neural crest cells (NCCs) form a population of cells that are derived from the ectoderm, found in early developing embryos, and are often referred to as a fourth germ layer because of their prominent role in tissue development. NCCs arise at the margin of the neural plate, as it forms crests that rise and meet to yield the neural tube. From this dorsal position they migrate individually or in small groups before their eventual differentiation into a diverse array of new tissues. Prior to migration, NCCs undergo an epithelial to mesenchyme transition (EMT) following interaction between the neural plate and the epidermis, after which they can begin migration from the neural tube to target locations as they respond to signaling mechanisms. During the transition, the cells' epithelial matrix properties are compromised with the tradeoff for the ability to adopt motile features. The transition makes the cell able to migrate from the epithelial surface as transcription factors are activated, cytoskeletal proteins are expressed, and the cellular basement membrane is degraded (Kalluir and Weinberg 2009). Tight junctions are disassembled by the down-regulation of occludins, structural proteins, and claudins, proteins that mediate $Ca^{2+}$ independent adhesions that are crucial for the function of a barrier in tight junctions (Sauka-Spengler and Bronner-Fraser 2008). Cell adhesion properties are incorporated following the EMT in order to allow NCC to efficiently migrate from one region to another. These include downregulating N-cadherin and

cadherin-6B in order to release cells so that they can follow along extracellular matrix molecules, such as fibronectin, laminin, and collagen that act as a scaffolding structure via the cell surface binding proteins, integrins and syndecans (Somaiah et al. 2015). However, the expression of cadherin-7, a type II cadherin, and integrin-β1 are all upregulated (Panda et al. 2001). In the chick embryo, the EMT occurs at HH stage 10-12 (Biechler et al. 2014).

During and after migration, the cells differentiate into many derivatives which can be grouped into two categories: ectomesenchymal (bone and cartilage) and non-ectomesenchymal (neurons, glia, and melanocytes) revealing the multipotent nature of these cells (Summarized by Gilbert 2010).

## Neural Crest Cell Migration Pathways

Neural crest cells follow specific pathways prior to differentiating. In the chick embryo, the recognition of specific pathways begins at gastrulation. Signaling molecules including BMPs (an acronym for bone morphogenetic protein) and Wnts (an acronym for Wingless-related integrated site of drosophila), induced at the future epidermis and border of the neural plate, are critical factors in determining the fate of cell progenitors into epidermis or neural crest cell tissue derivatives. Traveling to the first pharyngeal arch in the developing chick embryo are neural crest cells from the mid- and hindbrain, and from here they will follow specific signaling pathways in order to further differentiate. The second pharyngeal arch will fill with a population if NCCs that will differentiate into hyoid cartilage and bones of the middle ear. The third and fourth arches will contain NCC that will differentiate to parts of the thymus and thyroid glands as well

as cells that will develop into parts of the cardiac outflow tract (Kirby 1987; Waldo et al. 1998). A study done by Bockman and Kirby (1984) removed parts of the pharyngeal arches and found that the differentiating structures never developed; suggesting that the migration to these arches is a crucial step in order to further interact with their specific signaling stimuli (Bockman and Kirby 1984).

The BMP signaling pathway and Wnt pathway are known to be antagonists of each other; however, if the Wnt pathway induces BMPs, the cells will become neural crest. These induced cells will then express neural crest specifier genes, Pax7, Snail2, and Sox9 (Summarized by Gilbert 2010). In addition, it has been found that fibroblast growth factor-2 (FGF2) in combination with BMP can induce NCC migration by upregulating the transcription factor Snail2. The β-catenin dependent Wnt pathway, consists of a family of Cys-rich glycoproteins that play a significant role in the induction of cells traveling to develop the head, appendages, and heart. When the pathway is activated, β-catenin is stabilized due to an accumulation of Wnt molecules. β-catenin then becomes nuclear and interacts with a variety of transcription factors to up-regulate the expression of their downstream targets (Sauka-Spengler and Bronner-Fraser 2008). An experiment performed by Garcia-Castro and colleagues (2002) demonstrated that the Wnt signaling pathways alone is not only necessary for NCC induction and migration, but can also be efficient while acting as the only signaling pathway available (Garcia-Castro et al. 2002).

## Neural Crest Regions

The neural crest can be divided into five regions: cranial, cardiac, trunk, tail, and the vagal and sacral region of neural crest cells that originate from the hindbrain to the

caudal most point of the primary neural tube in an avian embryo. These regions will contain neural crest cells that will follow specific signals along migratory pathways resulting in the differentiation into varying cell types and tissues. The cranial neural crest cells will differentiate into cartilage, bone, cranial nerves, and connective tissues related to the face. These cells will also migrate into pharyngeal pouches where they can further differentiate into thymic cells, odontoblasts, and bones necessary to develop the middle ear and jaw (summarized by Gilbert 2010). Hox or Otx genes coordinate the migratory behavior of the cranial neural crest depending on whether or not a cell will express one of these genes. Hox genes are found in cells that create the hindbrain, parts of the jaw, and in cells that travel to locations within the pharyngeal arches. Cells containing Otx genes are seen in cells that contribute to the structure of the mandibular portion of the jaw and hyoid skeletal elements. Experiments performed by Noden (1993) involved a series of transplantations done prior to cell migration and resulted in cells expressing Hox genes maintaining their function of developing into hindbrain in the donor embryo, demonstrating the importance of cell differentiation specification in this neural crest region (Knight and Schilling 2000; Noden 1993).

Cardiac neural crest cells originate in a subregion of the cranial neural crest that extends from the ear placodes to the third somite pair (Kirby 1987). Cells of this region develop into melanocytes, neurons, cartilage, and connective tissue cells that compose the third, fourth, and sixth pharyngeal arches. Crucially, these cells also create the cardiac outflow tract of the embryonic heart, which consists of the muscular-connective tissue units of the large arteries as well as the septum that separates pulmonary circulation from

the aorta (Le Lievre and Le Douarin 1975). Several cardiac anomalies have been linked to the improper development of the outflow system involving neural crest lineage. The outflow system contains the aorticopulmonary septum (creating the pulmonary sac), the truncal septum (forming a partition between aortic and pulmonary semilunar valves, and the conal septum (which forms the closing unit involved in ventricular contraction). Cardiac neural crest cells are also known to play a role in forming the aortic arches via Hox gene information carried by these cells which will provide molecular cues for these structures to persist. Using chick ablation models, Creazzo and his team (1998) were able to explain the significance the cardiac neural crest has for heart development as well as the supporting structures necessary for healthy heart function (Creazzo et al 1998**).**

In addition, elevated homocysteine, an amino acid naturally found in the blood serum during development, has also been linked to cardiac anomalies. A review done by Rosenquist (2012) explains that when there is insufficient folic acid or vitamin B12, homocysteine levels increases and can be linked to increased risk for cardiovascular disease and congenital defects, especially defects that result from abnormal neural crest and neural tube development (Rosenquist 2012). Rosenquist and his team performed an experiment in which they looked at cardiac neural crest cells in vitro and then obtained RNA from the cultured cells to run a microarray analysis that compared homocysteine treated cells to untreated cells (controls). Their results showed that the amino acid is somehow interrupting normal neural crest cell activity by dysregulating certain transcription factors. The disturbance among these transcription factors has a direct

impact on the differentiation, migration, division capabilities, and survival of the cardiac neural crest cells (Rosenquist et al 2007).

NCCs also migrate to the eye during development and give rise to the cornea and ciliary body. Avian eye development is complex and requires, among many other steps, specific collagen arrangement between anterior epithelium and posterior endothelium layers in order to produce the cornea. Around the third day of chick embryo development, neural crest fibroblastic cells invade the anterior ocular region with its associated extracellular matrix macromolecules, such as hyaluronic acid. By day 6 of development, the cornea is evident and surrounded by layers of collagen (Bard and Higginson 1977). In an experiment by Svoboda and Hay (1987), the significance of collagen in the developing eye was investigated by disorganizing the rough endoplasmic reticulum (RER) so that the actin cytoskeleton could no longer mediate collagen production. They found that the disorganized RER produced less collagen, suggesting that binding of the RER to the actin cytoskeleton plays a significant role in creating the highly organized cell scaffolding structural collagen necessary for cornea development (Svoboda and Hay 1987). In an experiment by Gage and his team (2015), the significance of NCCs in eye development was highlighted by following cell migration in mammalian and avian models using recombinant transgenes with lineage markers counterstained to identify the expression of transcription factors associated with migrating NCCs. What they found is that there are several transcription factors expressed during ocular development that are key in understanding the migrating NCC and how they differentiate (Gage et al. 2015).

## Homocysteine

High levels of homocysteine (Hcys) have been linked to induction of neural crest cell differentiation by altering their cytoskeletal components and also by mitotic effects. It has been postulated that elevated levels of Hcys may alter DNA methylation; ultimately, altering early embryonic development and resulting in congenital heart defects. Elevated levels of Hcys have been associated with adult cardiovascular disease, birth defects, and can even have carcinogenic effects (Watkins et al. 2002).

Hcys is an amino acid found as a byproduct in the blood plasma. The metabolized product is a result of methionine activation to create S-adenosylmethionine, which then donates a methyl group. The loss of a methyl group creates S-adenosylhomocysteine. During a hydrolysis reaction, the final step yields homocysteine. This form of homocysteine can be metabolized two different ways: it can be remethylated into methionine or it can be converted to N-5-methyltetrahydrofolate and be used in the folate cycle or interact with vitamin B12 to convert to methionine again. This transfer system is carried out in the liver, kidneys, small intestines, and pancreas in the human model. Adequate uptake of folic acid will decrease the risk of neural tube and cardiovascular defects in the developing embryo by altering the metabolism of Hcys to provide to methyl groups. In addition, teratogenic effects of elevated Hcys have been reversed by folate supplementation (Milunsky et al. 1989). An error in this metabolic pathway can result in an accumulation of homocysteine that is transported directly to the blood causing hyperhomocysteinemia (Lai and Kan 2015).

In an experiment done by Boot et al. in 2003, neural tube explants were studied to observe behavior of cranial and cardiac NCCs exposed to 30µM or 300µM of L-homocysteine thiolactone hydrochloride; concentrations comparable to toxic amounts in a human model. They also observed explants exposed to a solution of 300µM of L-homocysteine thiolactone hydrochloride Hcys and 90µM folic acid. They found non-differentiated cardiac NCC in the Hcys only solutions as well as the higher (300µM) concentration of Hcys solution displayed neuroepithelial and NCCs both leaving the neural tube to attach to the fibronectin culture dish shortly after culturing in comparison to the control medium that saw loose attachment to the dish. In addition, the control explants did not express any cellular outgrowth whereas the more Hcys present in culture, the more outgrowth of NCCs from the neural tube; suggesting that Hcys is affecting the patterns and timing of migration of NCCs from this region. The alterations can be explained by an error in the EMT stage of differentiation which resulted in changes in cell motility, migration distance, and cell shape and size. However, when folic acid is present in the serum, the effects of Hcys were ameliorated; suggesting that folate plays a significant role on NCC migration and overall embryogenesis (Boot et al. 2003).

A study done by Brauer and Rosenquist (2002) looked at avian embryo developmental defects after they were injected with 10µmol of D,L-Hcys. They reported that 78% of the test subjects observed had statistically significant alterations with NCC migration, motility, cell area, and cell perimeter when compared to control embryos; which can ultimately lead to developmental defects (Brauer and Rosenquist 2002). In addition to direct effects of elevated Hcys, Rosenquist et al. (1996) performed an

experiment that determined a dose response effect of Hcys in blood serum in the avian model. The embryos were injected throughout a timed series with either 200mM D,L-homocysteine or 100mM L-homocysteine into an airspace in the amnion on incubation days 0, 1, and 2. They were harvested at 53 hours and it was found that 27% showed neural tube defects. To further the investigation of the dosage dependency on heart septation, embryos were injected with Hcys into their amnion on days 2, 3, and 4 of incubation. The embryos were harvested and analyzed after 9 days of incubation, when septation of the heart was complete. Of the surviving embryos, 23% showed ventricular septal defects and ventricular closure defects. When 45nmol/ml of folate supplement was added to the developing embryo, the teratogenic effect was not present (Rosenquist et al. 1996).

## The Folate Cycle

Folate is used as a collective short-hand term that includes a set of compounds that all act similarly in their biological activity (Ferre et al. 1990). Folic acid, however, is a fully oxidized synthetic compound commonly found in food products and as a dietary supplement. Upon ingestion, the oxidized form of folic acid is reduced using dihydrofolate reductase to its bioactive forms, tetrahydrofolic acid and methyltetrahydrofolate. Methyltetrahydrofolate is transported into cell via receptor mediated endocytosis where it can then use vitamin B12 as a cofactor in normalizing homocysteine levels in the blood serum by maintaining methylation levels of methionine via methionine synthase. Homocysteine is naturally found in the blood existing as an intermediate in the conversion of methionine to S-adenosylmethionine, also known as the

SAM product. This product can interact with coenzyme vitamin B6 in order to release cystathionine and convert Hcys to methionine again (Reviewed by Mahmood 2014).

In cases of folic acid deficiency, there is no source of methyl groups for production of methionine, resulting in low production of natural antioxidants and sulfur-containing amino acids, such as cysteine. Low levels of vitamin B12, B6, and folic acid have all been linked to congenital heart defects (Rosenquist 2012).

## Congenital Heart Defects

Congenital heart defects (CHD) are responsible for approximately 3% of infant deaths and affect roughly 7% of surviving infants (Zeng et al. 2016). There are several risk factors associated with CHD, including: genetic make-up, maternal alcoholism, and elevated maternal homocysteine levels due to insufficient folate or vitamins B12 and B6 in maternal blood serum, or dysfunctional enzymes (Megahed and Taher 2005). A study performed by Khong and Hague (1999) demonstrated that elevated embryonic homocysteine levels result in an embryo showing debilitating vascular changes such as vasodilation, thrombogenesis, infarction, or retroplacental hematomas. In addition, the homocysteine derived from methionine plays a significant role in cell proliferation and migration, and when levels are elevated, a migrating cell can experience cytotoxic effects (Khong and Hague 1999). There is evidence that the majority of CHD cases are correlated with two different causes: folate deficiency during pregnancy or defective cardiac neural crest and its relation to heart development (Reviewed by Rosenquist 2012).

Several studies that have employed restricted folate in the diet during pregnancy have been published during the past few decades. The first reports of deleterious effects on the cardiovascular system were published during the 1950's (Nelson et al. 1952; Baird et al. 1954). The largest of the effects were found in the cardiac outflow regions, including the aorta and pulmonary trunk (Monie and Nelson 1963). In addition to its other metabolic functions, folate drives mitosis because it delivers methyl groups for nucleotide synthesis. High mitotic capabilities require large amounts of folate relative to neighboring cells, both migratory and stationary. This is especially true for NCCs which proliferate rapidly and must also migrate to their specified location prior to entering S-phase of the mitotic cycle. Therefore, during the initial stages of NCC determination, pre-migratory cells express a high affinity for the receptor that recognizes folate intake and transport. When the receptor is perturbed, cardiac NCC migration is affected resulting in abnormal heart development, including conotruncal defects and reduced heart size (reviewed by Rosenquist 2012). Reduced maternal folate has also been linked to a change in DNA methylation due to the activity of the DNA-methyltransferase 3b (DNMT3b) enzyme. When the enzyme is experimentally knocked out, several neural crest genes responsible for their proliferation are either overexpressed or precociously expressed (reviewed by Martins-Taylor et al. 2012).

The positional identity of migrating NCCs is established by sets of transcription factors activated and deactivated throughout embryonic development. When signaling is blocked or interfered with because of environmental factors, NCC migration is affected

(Minoux and Rigli 2010). CHD can be directly related to a disturbance in cardiac NCC migration that creates the outflow tract of the heart.

## The CSRP-3 Protein

CSRP-3 is an acronym for "cysteine and glycine rich protein 3" and is part of the cysteine-rich protein family (CRP). This family of proteins is mostly found in the nucleus and along cytoskeletal components in the cytoplasm and play a significant role in tissue-specific cell growth and migration (Liu et al. 2016). The CRP family's cellular structure consists of tandem LIM zinc-finger domains followed by a paired glycine rich domain (Louis et al. 1997; Harper et al. 2000). This particular gene contains six exons and spans a 20-kb genomic region (Knoll et al. 2002). As a study done by Campos et al. (2009) comparing harvested smooth muscle cells from an in vivo system and rat endothelial cells in vitro explains that the primary stimulus for induction of CRP3 is stretch by. They found that CRP3 is found mostly in arteries, but is inducible in veins by of stretch. They found the stretch response to be more dependent in smooth muscle cells, as opposed to endothelial cells responding to stress in general (Campos et al. 2009).

CRP3 protein is encoded by the CSRP3 gene, which is expressed in both cardiac and smooth muscle, but most abundantly found in skeletal muscle (Arber et al. 1994). This gene encodes a transcription factor that plays an essential role in cell proliferation and differentiation, as well as acting as a regulator of myogenesis (Arber and Caroni 1996). CRP3 protein found in the cytoplasm can act as a scaffolding protein which interacts with structural proteins such as, α-actinin, and β-spectrin, in order to maintain actin-based structure of migratory cell (Kong et al. 1997; Konrat et al. 1997; Kontaxis et

al. 1998; Prassler et al. 1998; Kirchner et al. 2001). A study done by Knoll et al. (2002) shows that the Z-disc protein associated with stretch sensing are dependent on the CSRP-3 gene to prevent heart muscle contractile dysfunction and chamber dilation by observing mice that harbor a deficiency for the gene (Knoll et al. 2002).

In a microarray analysis performed by Rosenquist et al. (2007) comparing gene expression patterns of NCCs treated with elevated levels of homocysteine vs. no treatment controls, the CSRP-3 gene, part of the LIM protein family, was conspicuously elevated in mRNA expression, 177-fold (p value of 0.0005). Out of 68, it was one of only seven genes reported to show such striking elevation, and one of only two in the cell migration/adhesion group. This remarkable and provocative response to high Hcys merits further investigation. These results allow for the assumption that exposure to elevated homocysteine is directly correlated with impactful change in genes that have functions essential to cellular migration and differentiation, ultimately leading to major structural defects.

## Hypothesis

The Rosenquist et al. microarray study (2007) found over expressed CSRP-3 gene product in cultured cardiac neural crest region from a HH stage 10 embryo neural tube explant. This suggests that Hcys could lead to cardiac malformations by over-activating the CSRP-3 gene. Based on the findings from Rosenquist et al. (2007) and the understanding that development of the cardiac neural crest is influenced by NCCs and how they respond to Hcys levels, I examined and investigated NCCs in Hcys treated and untreated intact chick embryos. I evaluated quantitatively and qualitatively HH stage 10-

12 chicken embryos that allow to develop to HH stage 12-14 (about 48 hours old) for antibody fluorescence of NCCs expressing CSRP-3 protein. The embryos were injected with homocysteine into their amniotic sacks. If Rosenquist's findings in the 2007 study are true, there will be a more intense staining of positive cells in the treated embryos, compared to the control. In addition, I expected positive cells to be located throughout the entire cardiac neural crest region, including: the brain meninges, periocular region, paraxial mesenchyme, and the pharynx associated with the cardiac outflow tract. I used the NCC-specific antibody HNK-1 to identify and mark NCCs with a differently colored fluorescent tag, along with a nuclear stain to mark all cellular nuclei. This triple staining scheme coupled with high resolution and 3-D imaging capabilities of confocal microscopy allowed me to assess whether CSRP-3 protein itself is more highly expressed in whole and sectioned embryos where NCCs are migrating and developing in their natural context. NCCs in untreated embryos were compared to treated embryos in terms of cell fluorescence intensity, migration patterns, and population following the same protocol as the treated embryos.

# CHAPTER 2

# MATERIALS AND METHODS

## Culture and Fixation

Eggs from crossed New Hampshire Red/Plymouth Rock chicken were purchased from Sunray Hatchery (Hazelton, IA) or Mixdorf farms (Waterloo, IA). The eggs were incubated at 38˚C for 45-50 hours. Eggs were opened for viewing following a procedure modified from Dunn's shell-less culture technique (1991) by cracking the egg on a flat surface and opening it into a sterile sling made from Solo™ punch glasses, Saran Wrap™, sterile water, and a rubber band (figure 1A and B). The observable embryos were found to be between stages 10 and 12 (Hamburger and Hamilton 1951). To treat the exposed embryos, 1µl of a 200µM DL-homocysteine thio-lactone hydrochloride (ICN Biomedicals Inc.) dissolved in sterile Earl's balanced salt solution (EBSS) was injected into the embryo's amnion near the cranial flexure using a 1µl syringe (Hamilton Company Reno, NV). The sling structures were covered with plastic Petri dish lids and the injected embryos were allowed to incubate at 38˚C for 24 hours. After 24 hours, the embryos were removed from the yolk using 3MM filter paper rings. The excised embryo was rinsed briefly in EBSS before being transferred to a 20% DMSO (Dimethyl sulfoxide) in methanol fixative on ice. The embryos were allowed to fix for at least one hour, while remaining on ice.

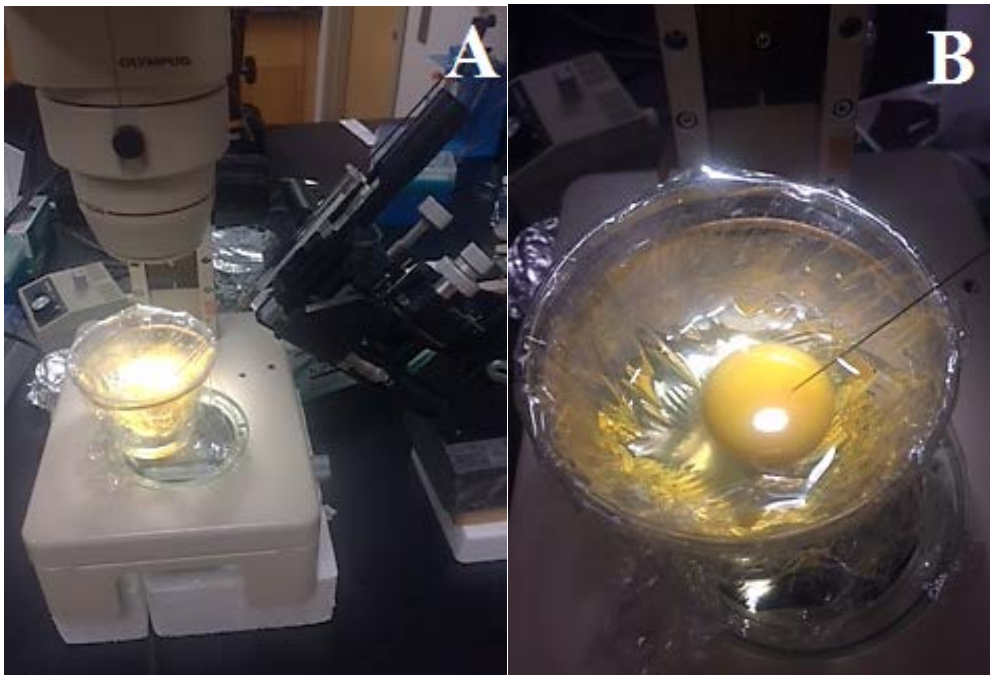


Fig 1. A) The set-up of the injection, with the embryo in the sling structure under the dissecting microscope, water is visible at the bottom of the sling. To the right is the 1µl syringe used to inject into the amnion. B) A closer view of an embryo prior to injection in the Solo punch glass, with a Saran Wrap sling created, held in place with a rubber band. To the right is the tip of the 1µl syringe aiming for injection

## Dehydration, Tissue Embedment, and Sectioning

Once fixation was complete, the explants were washed three times for five minutes each in a 1% phosphate buffered saline (PBS), which is composed of 4% NaCl, 0.1%KCl, 0.1% $KH_2PO_4$, 0.575% $NaHPO_4$, adjusted to a pH of 7.4. Following the rinses, the dehydration process began with 25 % ethanol, then 50%, 70%, 90%, and two 100% washes each for five minutes with agitation. Embryos were then transferred into a 1:1 Protocol Safeclear tissue clearing agent (Fisher Scientific) for five minutes with agitation, followed by a 100% Safeclear II™ wash for 10 minutes at 60˚C. The embryos were then transferred to a 1:1 solution of paraffin to Safeclear and allowed to infiltrate

overnight incubation at 60˚C. This was followed by a transfer to fresh 100% paraffin overnight incubation at 60˚C. The embryos were then removed from the paper rings and transferred to fresh paraffin and allowed to cool. The embedded embryos were mounted on wooden blocks and trimmed to present a trapezoid block face. They were then sectioned into either 6 or 10 µm thick slices using a Reichert-Jung Histocut 820 microtome. Sections were cut into ribbons 8-12 sections long and placed onto 45°C water beads on slides precoated with tissue section adhesive. The sections were allowed to adhere to slides on heat for at least one hour before the paraffin was removed.

Deparaffinization and Rehydration

Slides were deparaffinized in 100% Xylene, twice, and then into a 1:1 Xylene-ethanol mixture, followed by rinses in 100%, 90%, 70%, 50%, and 25% ethanol. They were then hydrated in deionized water, followed by a PBS rinse. All transfers were performed in Coplin jars for five minutes each with gentle agitation.

Immunohistochemistry of Sections

Sections were incubated overnight in blocking solution (0.5% bovine serum albumin, 1% Tween-20, and 1% non-fat dry milk in PBS) at 4°C overnight. Blocking solution was removed, and slides were rinsed three times in PBS for five minutes each with gentle agitation. Primary mouse monoclonal anti-CSRP3 antibody (Abcam, Cambridge, MA) diluted 1:100 in blocking solution was evenly applied to slides and then incubated overnight at 4°C. The monoclonal antibody was removed and slides were rinsed three times in PBS for five minutes each with gentle agitation. Detection of the primary antibody was done using goat IgG tagged with Alexaflour 488 (LifeTech) diluted

1:500 in blocking solution. Secondary antibody was applied to slides evenly and allowed to incubate overnight at 4°C.

NCCs were identified using HNK-1 primary antibody, a gift from Dr. Alicia Paulson at the University of South Dakota (collected at the American Type Culture Collection from hybridoma cell cultures) diluted 1:100 in blocking solution. The slides were incubated overnight at 4°C. The primary HNK-1 antibody was removed and slides were rinsed three times in PBS for five minutes each with gentle agitation. In order to detect the HNK-1 antibody, Alexafluor 594-tagged goat anti-mouse IgM (Jackson ImmunoResearch laboratories) diluted 1:500 in blocking solution was applied to slides and incubated at 4°C overnight. Slides were rinsed in deionized water for 3-5 seconds followed by staining in Dapi Flouromount-G mounting medium (SouthernBiotech). Slides were covered with a 22 X 50 X 1.5 coverslip and allowed to dry.

Immunofluorescence Staining of Whole Embryos

Whole embryos were injected and fixed following the same protocol used for embryos that were sectioned. After fixation, the explants were washed 3 times, 5 minutes each, in PBS with gentle agitation. The explants were then permeabilized in 0.1% Trition X-100 in PBS for 30 minutes with gentle agitation at room temperature. Whole embryos were incubated in blocking solution at 4°C overnight. This was followed by three PBS washes for 15 minutes each with gentle agitation.

Primary mouse monoclonal anti-CSRP3 antibody (Abcam) diluted 1:100 in 3% bovine serum albumin and 0.3% Triton X-100 (pH 7.4) was then applied to the embryos in a chamber to incubate overnight at 4°C. Embryos were then removed from the

antibody solution an washed 3 times in PBS for 15 minutes each prior to being submerged in secondary Alexaflour 488-tagged goat IgG (LifeTech) diluted 1:500 in 3% bovine serum albumin and 0.3% Triton X-100 (Ph7.4) overnight at 4°C in order to detect primary antibody. The embryos were washed three times in PBS for 15 minutes each before a second primary antibody application.

HNK-1 primary antibody diluted 1:100 in 3% bovine serum albumin and 0.3% Triton X-100 (Ph7.4) was applied and allowed to incubate overnight at 4°C. Alexafluor 594 conjugated goat IgM (Jackson ImmunoResearch laboratories) diluted 1:500 in 3% bovine serum albumin and 0.3% Triton X-100 (Ph7.4) was applied after three PBS washes, 15 minutes each, to identify NCCs, and allowed to incubate overnight at 4°C.

A 15-minute wash in PBS was performed, followed by a 5-minute wash in 70% ethanol, and another in 25% ethanol. The embryos were then submerged in a bisbenzimide solution (1mg/1ml in distilled water) for at least 2 hours in the dark at ambient temperature. The embryos were then washed in 70% ethanol for 5 minutes before being stored in fresh 70% ethanol.

## Image Analysis and Microscopy

Initial viewing of slide was done using a Leica DMIRE-2 inverted fluorescence microscope in order to identify fluorescence. Image analysis was then carried out using a Zeiss LSM 510 confocal microscope with 10x objective in combination with the Zen 2011 imaging software. Double and triple stained images were observed for confirmation of expressing NCCs, however, image analysis measurements were performed using only the 488 wavelength, which identified the transcription factor of interest. Stained cells'

fluorescence intensities were deciphered using the profile option while dragging the cursor across the desired cell area providing intensities in a range from 0-255. Background fluorescence was taken into account by dividing cell intensities by the average brightness values from 20 points across the neural tube.

Image analysis in 3-D of whole embryos was done using the Z stack option in the Zen software which compiled several images through the density of the embryo in order to display clusters of NCCs in three dimensions. Double and triple stained images of NCCs were constructed using the same wavelengths used with section analysis. Fluorescence average was not measured because it was not possible to view individual cells in the Z stack function.

# CHAPTER 3

# RESULTS

In this study, I searched for evidence that the amino acid homocysteine may cause cardiac malformations through its effects on gene regulation in migrating neural crest cells, in particular, the regulation of the transcription factor CSRP-3. NCCs are known to contribute to structural development in the embryo by migrating and differentiating once they have signals specifying their fate. I used specific antibodies to discover evidence at the protein level in NCCs that originate and migrate from five specific locations in 14 treated and 14 control embryos. NCCs within the paraxial mesenchyme, brain meninges, pharyngeal arches, and periocular regions are migratory and not yet differentiated at the time of Hcys injection, and can be identified using the NCC-specific HNK-1 antibody. CSRP-3 was localized using a monoclonal antibody and its fluorescence staining intensity was calculated using imaging software that directly measures fluorescence.

## Antibody Specificity and Staining Consistency

HNK-1 is a monoclonal antibody that was initially raised against quail ciliary ganglion cells and human leukemic cell lines, but has been found to recognize the same epitope on neural crest cells in the chick embryos, after they have become migratory (Del Barrio and Nieto 2004; Loring and Erickson 1987). It recognizes a carbohydrate group that is common among cell adhesion molecules found on melanocytes, and neurons in some ganglia found in the central nervous system (Mica et al. 2013). Double staining was performed using HNK-1 and CSRP-3 antibody to identify early migratory neural crest cells. Using double staining techniques described in the methods section, we were

able to scan images with two different wavelengths in order to recognize both the CSRP-3 protein staining green and HNK-1 positive cells staining red. Cells expressing both proteins at the same location were distinguished by their white fluorescence colocalization that was distinct from the green and red fluorophores used to localize CSRP-3 and HNK-1, respectively

Autofluoresence of Erythrocytes

Red blood cells exhibit fluorescence as a result of accumulation of conjugated Schiff base compounds derived from lipid peroxidase and amino groups resulting from oxidative stress (Stoya et al. 2002). I observed this as very bright autofluorescence from erythrocytes within blood vessels and occasionally from cells outside of them. Therefore, it was important to distinguish erythrocyte autofluorescence from the immunofluorescence signal coming from bound secondary antibodies.

Figure 2A displays an area known to carry erythrocytes, the dorsal aorta with an area that is not known to have a direct source supplying blood; however, during the embryo removal prior to fixation spillage of blood cells can occur. In comparing fluorescent cells visible in Figure 2A to those visible in Figure 2B, it is evident that blood cells are larger and have a disc shape while NCC's have an irregular shape due to their migratory behavior. Erythrocytes also display a different fluorescence pattern, with intensity values much greater than those of NCC's.

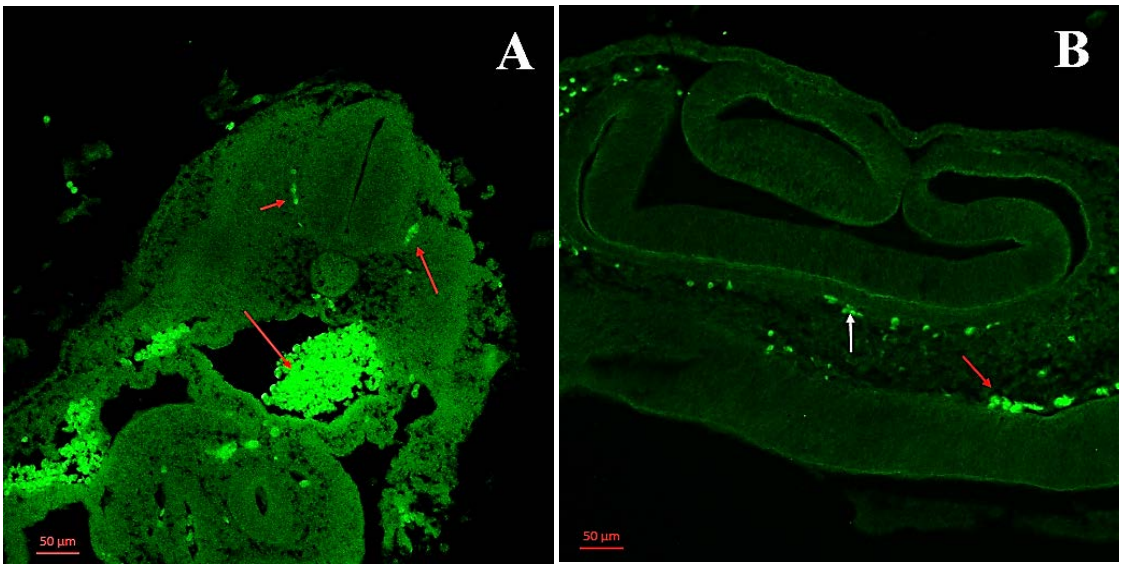


Fig. 2. A) A no primary antibody control cross section through the paraxial region revealing the simmilarities between blood cells within cardinal veins along the neural tube, and blood cells in the dorsal aorta. Red arrows indicate blood cells. B) A cross section of the periocular region of an EBSS injected embryo revealing the difference between neural crest cells and blood cells. White arrow indicates CSRP-3 expressing neural crest cells. The red arrow indicates red blood cells.

## Homocysteine Increases the Number of CSRP-3 Expressing Cells

Homocysteine is known to alter the patterns and efficiency of migration of NCCs, such that cells migrating to the cardiac region may be mis-timed (Brauer and Rosenquist 2002). In this study, chick embryos injected with Hcys at HH stages 10-12 and then examined 24 hours later were found to have greater numbers of CSRP-3 positive cells when compared to EBSS injected embryos (Table 2). Collectively, 65% of the CSRP-3+ NCCs counted were exposed to elevated amounts of Hcys.

Table 1. Comparison of cells counted that were expressing CSRP-3 transcription factor from 14 HH stage 10-12 EBSS injected chick embryos and 14 HH stage 10-12 Hcys injected chick embryos

| Region | No. of CSRP-3 positive control cells counted | No. of CSRP-3 positive treated cells counted |
|---|---|---|
| Brain Meninges | 96 | 208 |
| Paraxial Mesenchyme | 169 | 251 |
| Periocular Mesenchyme | 210 | 333 |
| Pharynx Region | 47 | 179 |

Homocysteine Augments CSRP-3 Expression Among NCCs of the Brain Meninges

The brain meninges are formed from migratory NCCs during the developmental period that was studied, and it was of interest to determine whether the CSRP-3 transcription factor would be expressed in these cells, and if so, whether Hcys would affect the level of expression. As seen in Figure 3, background was relatively low with obvious stained cells in both images. These cells clearly expressed CSRP-3 at varying levels of brightness, and formed a continuous membrane that surrounded the diencephalon and other brain segments. Most of these cells also expressed HNK-1, as revealed in double staining experiments.

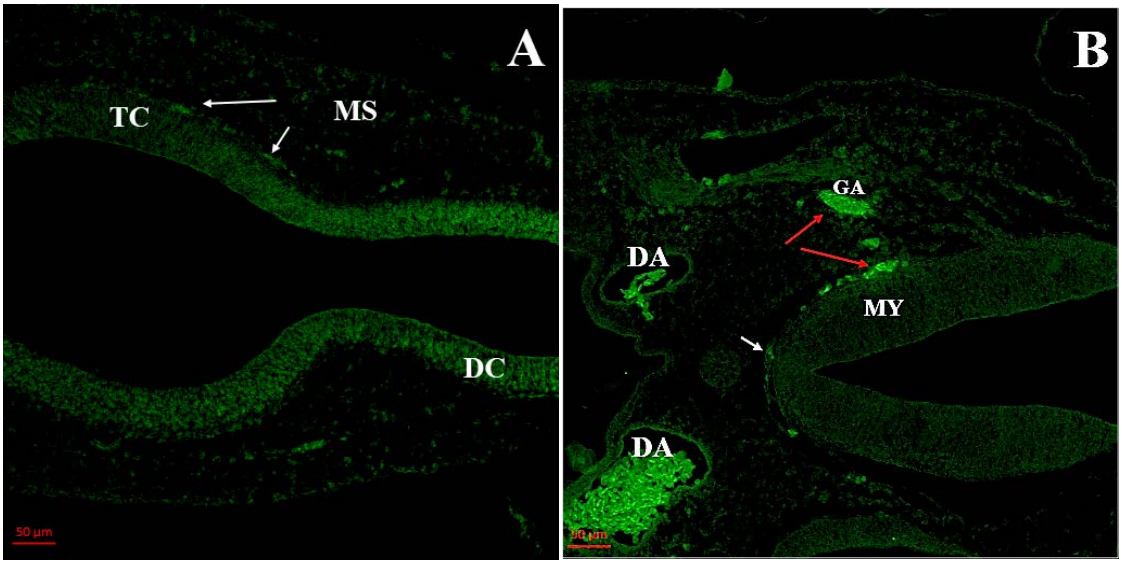


Fig. 3. A) Anti-CSRP-3 stained cross section of the brain of an EBSS injected HH stage 13-14 embryo. White arrows indicate NCC clusters along the brain in the meninges with an intensity ratio of 3.1. TC – Telencephalon. DC – Diencephalon. MS – Mesenchyme. B) A cross section of the brain of Hcys treated HH stage 11-12 embryo. Stained with anti-CSRP-3. Red arrows indicate blood cells; white arrow indicates CSRP-3 positive NCCs with an intensity ratio of 7.4. MY – Mesencephalon. DA – Dorsal aorta filled with autofluorescent blood cells. GA – Spinal Ganglion.

Because the intensity of anti-CSRP-3 stained NCCs showed apparent variability, it was of interest to determine the frequency distribution of the intensity ratios that we measured. Therefore, we plotted these values to create a histogram (Fig. 4). The statistical distribution was found to be not normally distributed but were instead strongly skewed with much greater representation of highly intense cells. This may be because the detector was unable to distinguish differences near or above its maximum measurement value. As a result of the skewed distribution, we compared the Hcys-treated and control cell intensity ratios using treated and non-treated cells were compared using the Wilcoxon Rank Sum Test. The skewed distribution in intensity was found to be present in all tissue regions included in the study. To characterize the differences found to

result from Hcys treatment, we constructed boxplots showing median, minima, maxima, and quartiles to reveal the magnitude and significance of differences resulting from treatment (Fig. 5). For the embryonic brain meninges that we analyzed, it was clear that Hcys treatment increased staining intensity, nearly doubling the median intensity ratio.

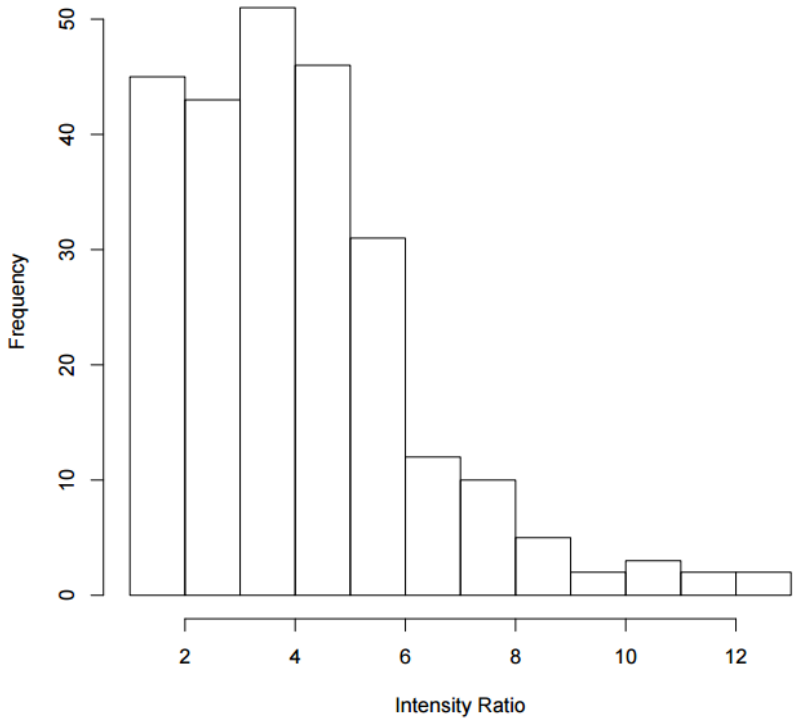


Fig. 4. A histogram revealing the distribution of intensity ratio values for Hcys treated cells expressing CSRP-3 in the brain meninges of stage 11-14 chick embryos. The distribution shows a much higher frequency of high intensity cells.

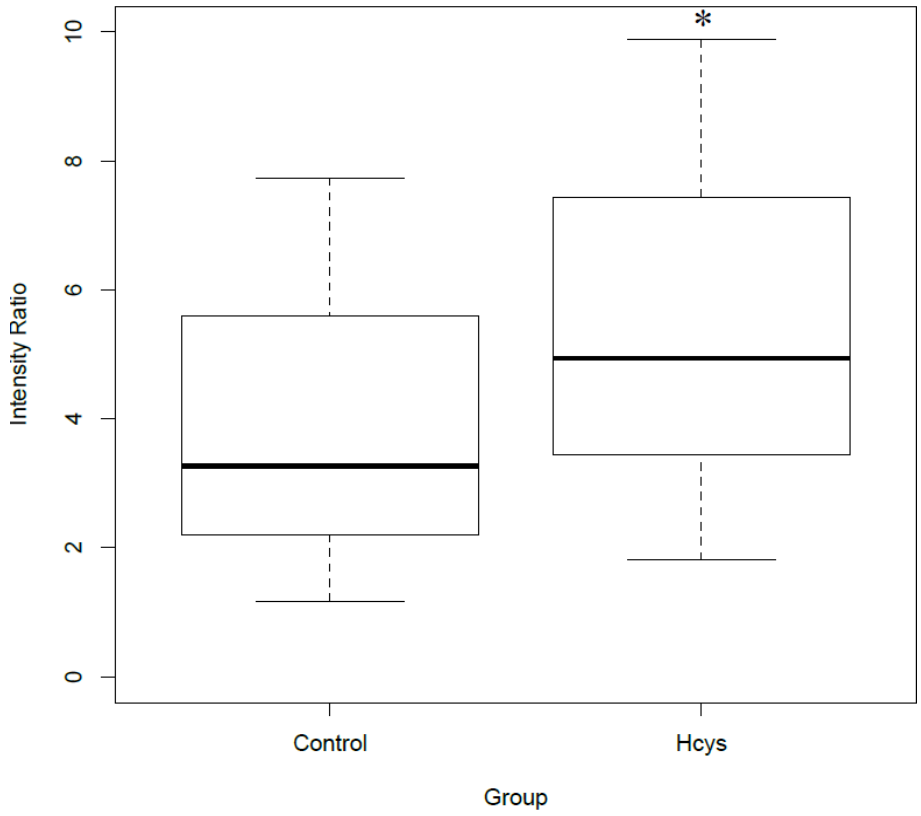


Fig. 5. A boxplot depicting the corrected fluorescence intensity of the Hycs treated cells compared to EBSS (control) injected cells in the brain meninges of stage 11-14 chick embryos. The heavy line indicates the median, top and bottom lines represent the first and third quartiles, and the whiskers show minima and maxima.
*Hcys cells were significantly greater than EBSS treated cells (control), with a P-Value of <2.2e-16.

Homocysteine Augments CSRP-3 Expression Among NCCs of the Paraxial Mesenchyme

The paraxial mesenchyme flanking the hindbrain and spinal cord is a significant a region for NCC migration containing cells that will give rise to neurons, melanocytes, glia, and connective tissue cells. I analyzed this region to look for CSRP-3 expressing cells and to examine the effect of Hcys on fluorescence intensity ratios. I discovered many cells in a scattered pattern, some quite near the neural tube, some present in early

forming ganglia, and some scattered laterally. Fig. 6 displays these findings, and also illustrates two sections of clearly differing background fluorescence that could nevertheless be compared in fluorescence intensity ratio.

As seen in Fig. 6A, the background fluorescence for EBSS injected cells (controls) was brighter than that of Hcys treated cells (Fig. 6B). This was corrected by dividing the average neural tube background intensity in each image from measured cells.

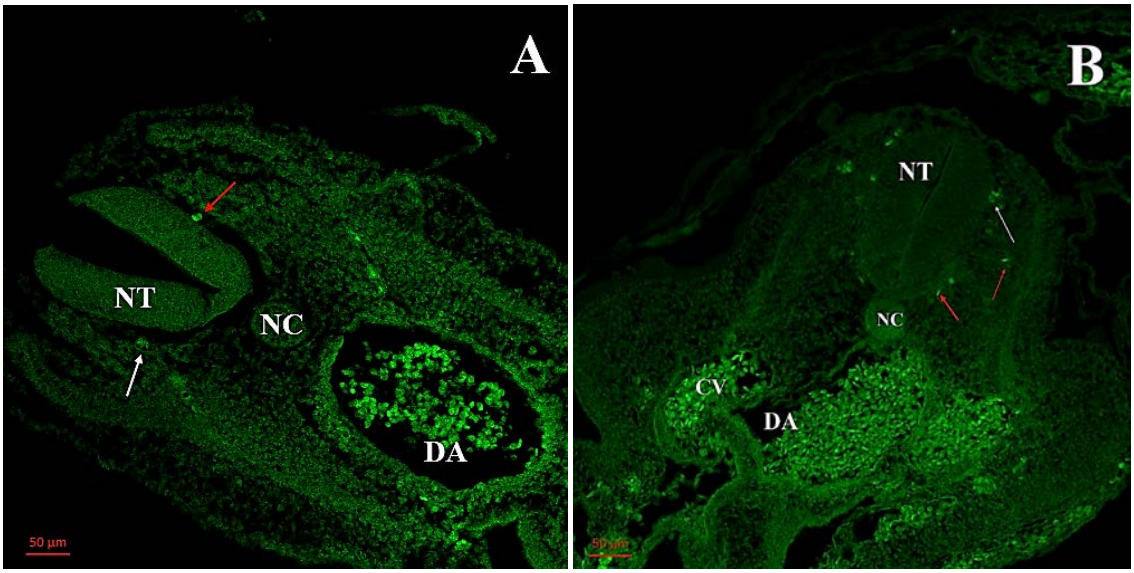


Fig. 6. A) A cross section of the paraxial mesenchyme region an anti-CSRP-3 immunostained control HH stage 11-12 embryo. Red arrows indicate blood cells and the white arrow indicates CSRP-3 positive neural crest cells with an intensity ratio of 2.0. NT – Neural Tube. NC – Notochord. DA – Dorsal aorta. B) A cross section of an anti-CSRP-3 primary antibody and fluorescent secondary antibody paraxial mesenchyme in a Hcys injected HH stage 12-13 embryo. The white arrow indicate CSRP-3 positive neural crest cells accounted for in the study with an intensity ratio of 5.5. Red arrows indicate red blood cells not accounted for in the study. This image clearly shows that background staining was lower than in image A, yet the CSRP-3 positive cells are of about equal brightness. NT – Neural Tube. NC – Notochord. CV – Cardinal Veins. DA – Dorsal aorta. PH – Pharynx.

It was apparent that the ratios were higher in Hcys injected embryos, which was revealed using boxplots (Fig. 7) showing median, minima, maxima, and first and third

quartiles. Due to the non-normal distribution of the data, difference between controlled and Hcys treated embryos was tested using the Wilcoxon rank sum test. The test showed that the difference was highly significant (Fig. 7) illustrating p-value on the boxplot.

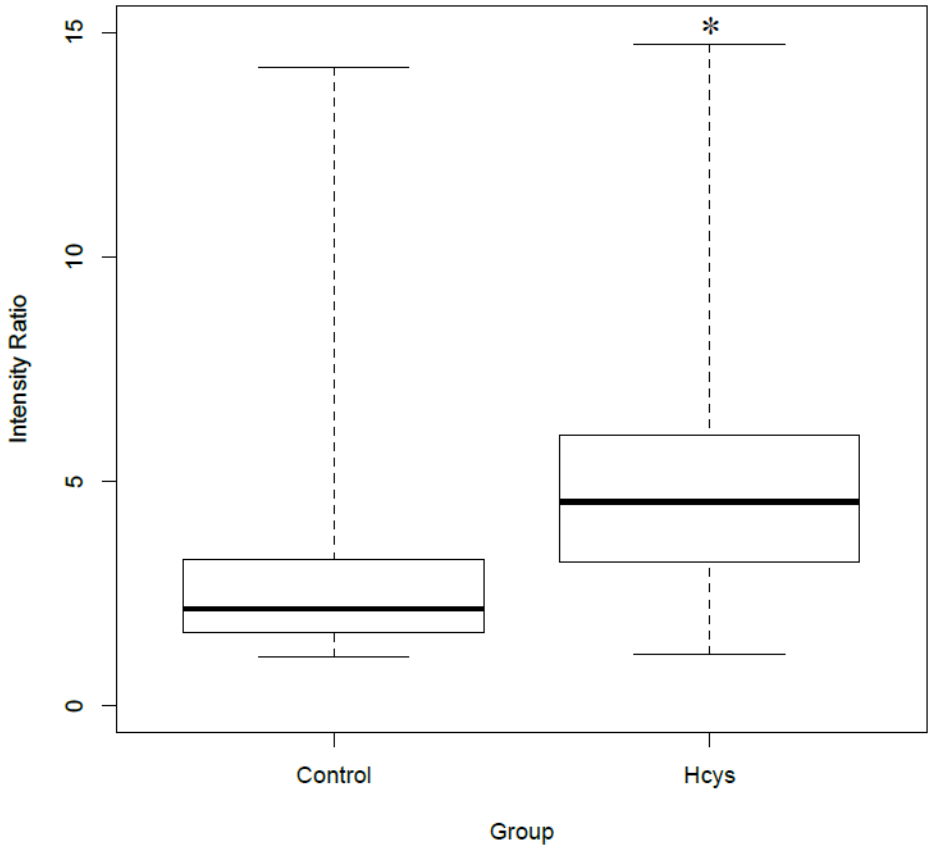


Fig. 7. A boxplot of fluorescence intensity ratios intensity of CSRP-3 immunostained NCCs in the paraxial mesenchyme region of the anterior trunk. Hcys treatment clearly enhanced CSRP-3 immunostaining intensity.
*Hcys embryos were found significant over controls with a P Value of <2.2e-16.

## Homocysteine Augments CSRP-3 Expression Among NCCs of the Periocular Region

The head mesenchyme near developing eyes, referred to as the periocular mesenchyme, contains abundant migrating NCCs. They will form the corneal precursor

cells and associated collagen fibers. These cells migrate into the region between corneal epithelium and lens vesicle. They will eventually generate the avascular, curved, transparent cornea. I analyzed these cells for NCC identity and CSRP-3 expression and found that 63% of Hcys treated cells were positively expressing both the transcription factor and the HNK-1 antibody. Representative sections are displayed in Figure 8. It is evident that the background fluorescence was similar in control (A) and Hcys-treated (B) embryo sections. Yet Hcys treatment clearly elevated the apparent brightness of stained cells. This difference was confirmed by calculating fluorescence intensity ratios and comparing them using box plots (Fig. 9). In Figure 8C, a section used for a control with neither primary antibody was stained with only secondary antibodies and DAPI to identify nuclei. No CSRP-3 expressing cells were found present in these sections.

Figure 8D is a Z-Stack image created using the Zen software through several layers of the embryo to examine three-dimensional aspects of the effect of Hcys on NCC expression of CSRP-3. One such image which was double stained using both antibodies displays the periocular region and is shown in Fig. 8D. The circled area highlights positive NCC staining as well as white, double stained, cells migrating through and around the optic cup.

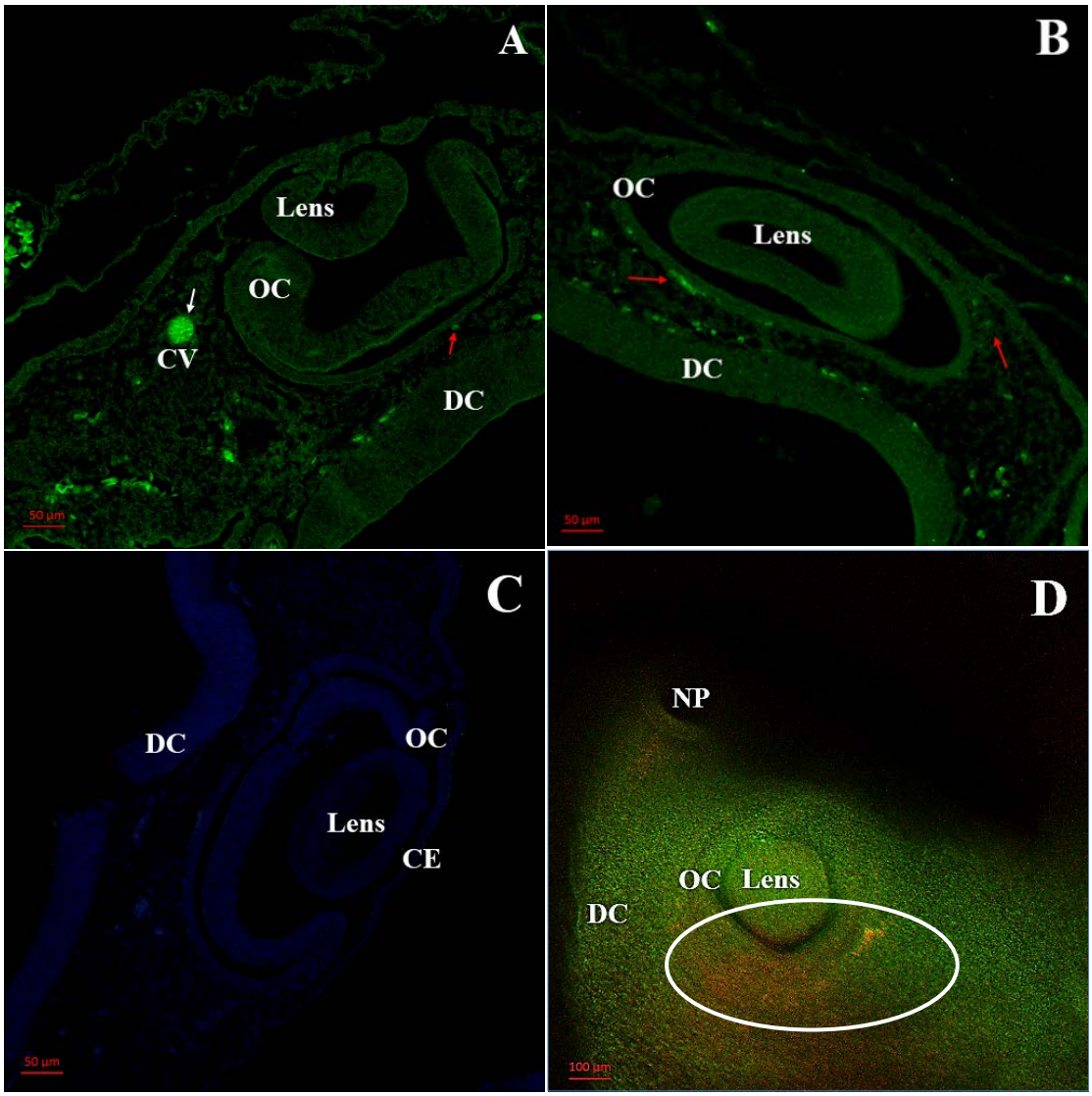


Fig. 8**.** A) The periocular region of a control HH stage 14 embryo stained for the CSRP-3 transcription factor. The red arrow specifies positive CSRP-3 NCCs present in the mesenchyme with an intensity ratio of 4.7 and the white arrow identifies a cluster of RBCs. OC – Optic Cup. DC – Diencephalon. CV – Cardinal Vein. B) The periocular region of a Hcys injected HH stage 13-14 embryo stained for CSRP-3. The red arrows indicate clusters of CSRP-3 positive NCCs with an averaged intensity ratio of 6.6. OC – Optic cup. DC – Diencephalon. C) Section through a control embryo used as a staining control. It was stained with DAPI to reveal nuclei but primary antibody was omitted. The section revealed very little non-specific binding of the CSRP-3 antibody and no staining of migrating cells. DC – Diencephalon. OC – Optic Cup. CE – Cornea Epithelium. D) Image of a Hcys injected, triple stained, three-dimensional Z stack of a HH stage 12-13 embryo. The circle surrounds "white" cells that expressed both CSRP-3 (green) and HNK-1 (red). The cells give the appearance of migration through the cranial and periocular region towards the eye. NP – Nasal Placode. DC – Diencephalon. OC- Optic Cup. In this orientation anterior is to the left and ventral is up

The intensity ratio data associated with the periocular mesenchyme is depicted in Figure 9, revealing that Hcys treated embryos expressed approximately 2.5-fold higher fluorescence. Statistically, the two groups were compared using the Wilcoxon rank sum test, which revealed that Hcys embryos showed significantly greater intensity ratios.

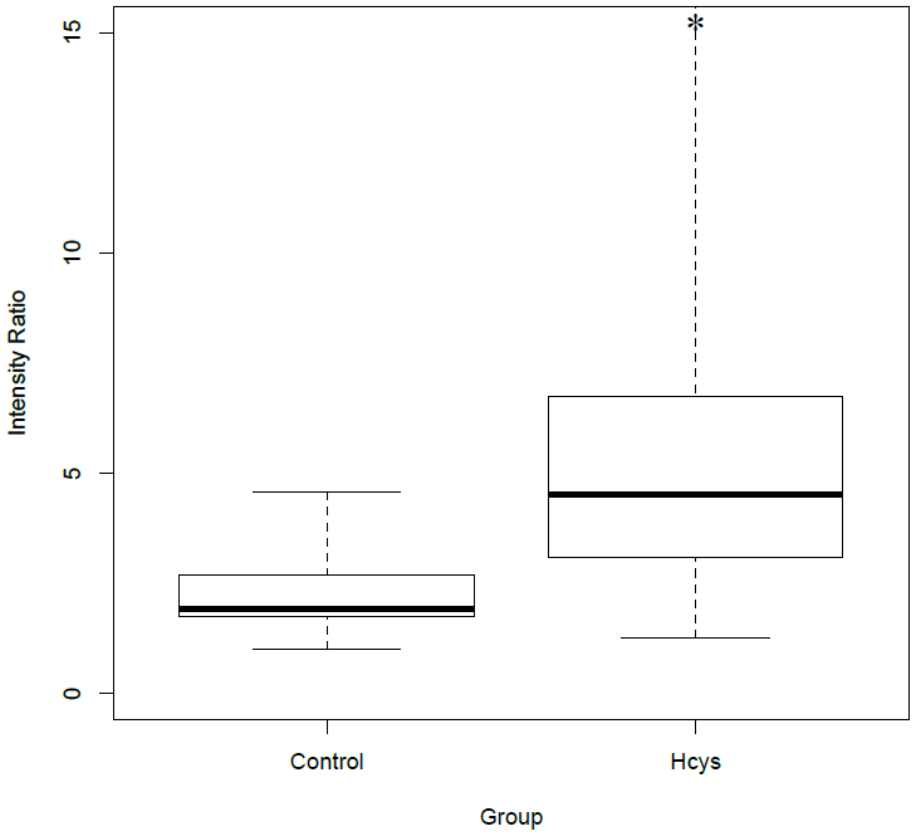


Fig. 9. A boxplot of corrected fluorescence intensity of CSRP—3 immunostained NCCs seen in sections of the periocular mesenchyme. Hcys injected embryos revealed NCCs with much greater CSRP-3 intensity.
*Hcys injected embryos were found to be significantly greater than the control with a P Value of 1.928e-15.

Homocysteine Augments CSRP-3 Expression Among NCCs of the Pharynx

Cardiac neural crest cells migrate through the pharynx into the first four pharyngeal arches. In particular, the NCCs migrating through the third and fourth arches will differentiate into parts of the thymus and thyroid glands, as well as parts of the cardiac outflow tract as they continue beyond the pharynx. Thus the "cardiac neural crest cells" migrate here. There were fewer sections with identifiable, positively stained cells in this region compared to other regions. This may be a function of the age of development at which the embryos were dissected. According to the atlas of Bellaris and Osmond (2005), development of the pharyngeal region is not complete until embryonic stage 16, and NCCs will not migrate down into this region until stages 13-14 (Bellaris and Osmond 2005). Of the cells I was able to observe in the pharynx region, Hcys treatment resulted in significantly greater intensity when compared to cells in EBSS injected embryos (Fig. 11). Figure 10C shows a no primary antibody control with no CSRP-3 staining cells present. A Z-Stack image created using the Zen imaging software through the pharynx of a whole embryo is shown in Figure 10D. I was able to observe stained cells in three dimensions in the expected location for cardiac neural crest cells. The circled region surrounds white colored cells migrating into the second pharyngeal arch. Third and fourth arches did not reveal any white cells, possibly due to the age of development of the observed embryo.

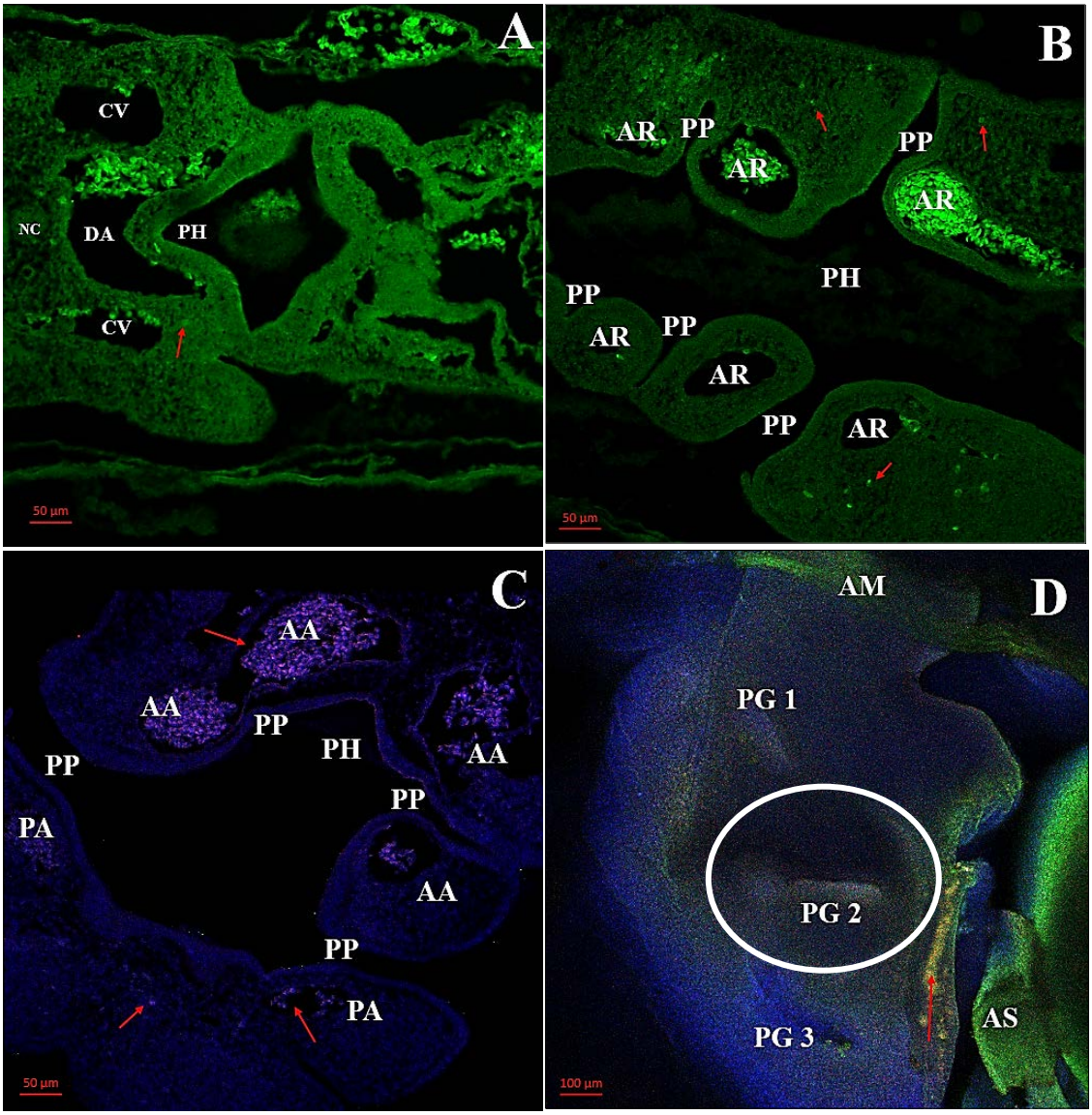


Fig. 10. Sections (A-C) and a 3D Z stack (D) image of control and Hcys treated chick embryos immunostained for CSRP-3. A) The pharynx region of a HH stage 11-12 chick control embryo. The red arrow indicates CSRP-3 positive cells with an intensity ratio of 1.7. CV- Cardinal Veins. DA- Dorsal Aorta. NC- Notochord. PH- Pharynx. B) The pharynx region of a HH stage 13-14 chick embryo injected with Hcys. Red arrows point to positive CSRP-3 cells with an intensity ratio of 3.6. AR- aortic arches. PP – Pharyngeal pouches. PH- Pharynx. C) A section through the pharynx of an EBSS injected, no primary antibody control region of a HH stage 11-12 chick embryo pharynx; the section shows no fluorescence of the CSRP-3 transcription factor. Red arrows indicate stained blood cells. AA – Aortic Arch 1-3. PP- Pharyngeal pouch 1-3. PA – Pharyngeal arch. PH- Pharynx. D) 3D Z stack image of a Hcys injected, triple stained, HH stage 12-13 embryo. The circle surrounds “white” cells that express both CSRP-3 and HNK-1 apparently migrating through pharyngeal arches towards the heart. The red arrow indicates blood cells that have been triple stained. PG – Pharyngeal Groove 1-3. AM – amnion. AS- Aortic Sac.

Cells treated with Hcys were not only brighter, but also showed higher fluorescence intensity ratios than controls, and difference was significant (Fig. 11). The median was closer to that of the control sections in the pharynx region, however, the measured Hcys treated cells were still found to be approximately 1.5-fold higher, which was a significant difference. This may be due to due to slower maturation of pharyngeal NCCs based on the age of the embryos.

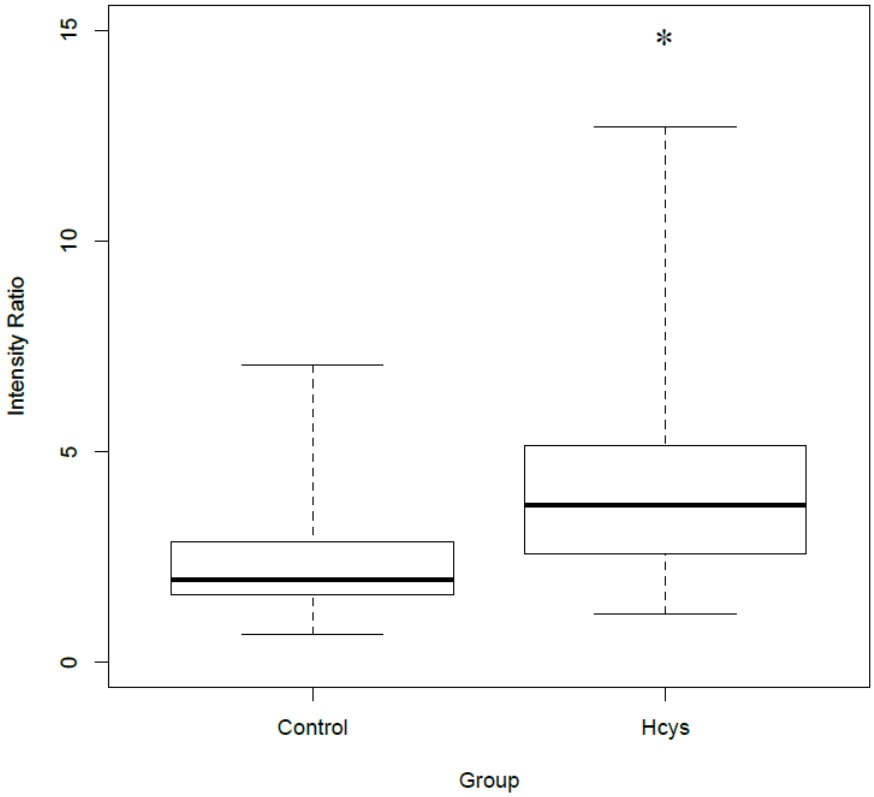


Fig. 11. A boxplot highlighting the corrected CSRP-3 fluorescence intensity ratio difference between EBSS (control) injected embryos and Hcys injected embryos in the pharynx region. Hcys treatment greatly augmented staining intensity.
*Hcys injected embryos were found to be significantly greater than the control with a P Value of 4.662e-8.

## Summary and Testing of CSRP-3 Fluorescence Intensity Ratios in Four Embryonic Tissue Regions

The distribution of fluorescence intensity among all regions analyzed in the embryos was found to be not normally distributed. Therefore, it was statistically analyzed for significance using the Wilcoxon-Rank Sum test as well as plotting the medians into boxplots. The p-values calculated from testing provided (Table 3) confirm that the intensity ratios of Hcys treated cells to that of EBSS treated cells were significantly increased in all four tissues analyzed.

Table 2. Results of Wilcoxon Rank Sum Test including P-Values

| Location | Wilcoxon Sum | P-Value |
|---|---|---|
| Brain Meninges | 9533 | <2.2e-16 |
| Paraxial Mesenchyme | 14838 | <2.2e-16 |
| Periocular Mesenchyme | 988 | 1.928e-15 |
| Pharynx Region | 5968 | 4.662e-8 |

# CHAPTER 4

# DISCUSSION

Homocysteine is an amino acid found naturally in the blood plasma as a crucial player in the folate cycle. When the cycle is irregular, the Hycs groups can accumulate in the blood causing hyperhomocyteinemia which directly effects migrating behavior of neural crest cells by altering their cytoskeletal components necessary to migrate and differentiate (Rosenquist 2012). Specifically, individuals with cardiac neural crest cells that fail to migrate into the third and fourth pharyngeal arches will acquire heart defects due to a lack of septation and formation of the outflow tract for which differentiated NCC's are responsible. In a microarray analysis explaining the effects Hcys has on mRNA expression of known genes performed by Rosenquist et al. (2007), coding for proteins involved in cellular adhesion and migration was shown to be altered. One of the gene products most increased was found to be a LIM domain protein symbolized as CSRP-3, which was upregulated to 177 times above control level (Rosenquist et al. 2007). In this study, I injected HH stage 10-12 embryos with Hcys and using antibodies compared CSRP-3 protein expression to that in saline (EBSS) injected controls. The injection was entered into the amnion in the cranial region of the developing embryo. Neural crest cell migration begins at the dorsal neural tube starting around HH stage 6; so at the stage of injection, NCC migration is well underway (Debby-Brafman et al. 1999). CSRP-3 expressing NCCs were observed using fluorescence microscopy (including 3D Z-stack imaging) and comparing fluorescence intensity ratios from immunostaining between Hcys treated embryos and EBSS (control) treated embryos. A monoclonal anti-

CSRP-3 primary antibody was used in conjugation with a secondary fluorescent tagged antibody to identify CSRP-3 expressing cells. HNK-1 was used as the primary antibody followed by a secondary antibody tagged with a different color to identify neural crest cells. Cells that expressed fluorescence for both antibodies were those of interest.

For analysis, three embryonic regions, in addition to the pharynx region (which contains the cardiac NCC migration pathways), were chosen based on their abundance of NCCs and their significance in organ and supporting structure development. This strategy gave context for comparison to the cardiac NCC region, and also gave new information. These regions were the mesenchyme forming the brain meninges, the paraxial regions along the spinal cord and hindbrain, mesenchyme surrounding the optic cup. Primary antibody labeling in this study was found to be specific based on staining controls, and did conform to predictable NCC patterns. We found that many mesenchymal cells did not stain with HNK-1 but were positive for CSRP-3. These cells may represent a small subpopulation of NCCs not expressing the HNK-1 epitope. Alternatively, they represent non-NCCs differentiating along a common pathway to form similar cell types.

Along the brain meninges, more than 68% of the cell population was found positive when injected with Hcys as well as expressing a more intense fluorescence when compared to EBSS exposed NCCs. This suggests that Hcys is causing higher and more widespread CSRP-3 expression. The results shown support the initial hypothesis that elevated levels of Hcys in the blood serum will result in over expression of the CSRP-3 transcription factor in regions like the meninges, in addition to the cardiac neural crest

cell region. Notice the statistically significant p-values shown in table 2. In addition, our data results affirm what the microarray results of Rosenquist et al. (2007) would predict, that Hcys elevates CSRP-3 protein as well as mRNA, and they demonstrate that the effect of Hcys occurs in living embryos.

The NCCs identified along the paraxial mesenchyme also supported the proposed hypothesis, such that they were found to be significantly brighter and more abundant in the presence of Hcys with approximately 60% of cells being injected with Hcys (Table 2) than those of EBSS injected embryos.

Neural crest cell fluorescence intensity ratios along the periocular mesenchyme of Hcys treated embryos were significantly brighter and abundant with more than 61% of cells counted injected with Hcys (Table 2), supporting the initial hypothesis. The number of cells present seemed to depend on the stage of development, suggesting that elevated Hcys levels during migration waves will affect more cells in different regions at different times. Based on microscopic images, the older the embryo, the more NCCs found near the optic cup and not the paraxial mesenchyme.

There were fewer embryos in which we found HNK-1 positive NCCs in the pharynx region compared to the other three regions. However, those that did have positive cells revealed that again, Hcys treatment caused significantly brighter fluorescence than in control embryos with more than 79% of cells counted being exposed to Hcys (Table 2), supporting the proposed hypothesis. The consistency of increased cell numbers in all 14 Hcys treated embryos compared to the 14 EBSS injected control embryos is provocative, and it supports the findings of Boot et al. (2003) using neural

tube explants to study NCC behavior when exposed to varying concentrations of Hcys. They reported that in the presence of Hcys, cell migration is occurred too rapidly and was inefficient, resulting in cardiac defects (Boot et al. 2003).

The findings of this study support and extend Rosenquist et al.'s (2007) using microarray analysis of cultivated neural crest explants. Furthermore, the findings support the hypothesis advanced by Rosenquist (2012) that proposes that congenital heart defects and neural tube defects are linked directly to errors in the folate cycle, particularly those that lead to hyperhomocysteinemia (Rosenquist 2012). In the Rosenquist et al. (2007) study, the expression of CSRP-3 mRNA was upregulated 177 fold in the presence of Hcys. This investigation supports and extends the cellular model of Rosenquist et al (2007).

# REFERENCES

Arber S, Caroni P. Specificity of single LIM motifs in targeting and LIM/LIM interactions in situ. Genes Development. 1996; 10: 289-300.

Arber S, Halder G, Caroni P. Muscle LIM protein, a novel essential regulator of myogenesis, promotes myogenic differentiation. Cell. 1994; 79: 221-231.

Baird C, Nelson M, Monie I, Evans H. Congenital cardiovascular anomalies induced by pteroylglutamic acid deficiency during gestation in the rat. CircRes AHA Journals. 1954; 11:544–554.

Bard J, Higginson K. Fibroblast-collagen interactions in the formation of the secondary stroma of the chick cornea. The Journal of Cell Biology. 1977; 74: 816-827.

Bellairs R, Osmond M. The Atlas of Chick Development, 2nd Edition. Academic Press. Cambridge (MA); 2005.

Biechler S, Junor L, Evans A, Eberth J, Price R, Potts J, Yost M, Goodwin R. The impact of flow-induced forces on the morphogenesis of the outflow tract. Frontiers in Physiology. 2014; 5: 1-14.

Bockman D, Kirby M. Dependence of thymus development on derivatives of the neural crest. Science. 1984; 223(4635): 498-500.

Boot M, Steegers-Theunissen R, Poelmann R, Van Iperen L, Lindemans J, Gittenberger-de Groot A. Folic acid and homocysteine affect neural crest and neuroepithelial cell outgrowth and differentiation in vitro. Developmental Dynamics. 2003; 227: 301–308.

Brauer, P, Rosenquist T. Effect of elevated homocysteine on cardiac neural crest migration in vitro. Developmental Dynamics. 2002; 224(2): 222-230.

Campos L, Miyakawa A, Barauna V, Cardoso L, Borin T, Dallan L, Krieger J. Induction of CRP3/MLP expression during vein arterialization is dependent on stretch rather than shear stress. 2009; 140-147.

Creazzo T, Godt R, Leatherbury L, Conway S, Kirby M. Role of cardiac neural crest cells in cardiac development. Annual Review of Physiology. 1998; 60(1): 267.

Debby-Brafman A, Burstyn-Cohen T, Klar A, Kalcheim C. F-Spondin, expressed in somite regions avoided by neural crest cells, mediates inhibition of distinct somite domains to neural crest cell migration. Neuron. 1999; 22: 475-488.

Del Barrio, Nieto M. Relative expression of Sluug, RhoB, and HNK-1 In the cranial neural crest of the early chicken embryo. Developmental Dynamics. 2004; 229(1): 136-139.

Dunn B. Methods for shell-less and semi-shell-less culture of avian and reptilian embryos. Egg Incubation: its effects on embryonic development in birds and reptiles. 1991: 409-418.

Ferre J, Jacobson K, Pfliederer W. Proposal towards a normalization of Pterdine nomenclature. Pteridines. 1990; 2: 129-132.

Gage P, Rhoades W, Prucka S, Hjalt T. Fate Maps of Neural Crest and Mesoderm in the Mammalian Eye. Ivos. 2015; 46: 4200-4208.

Garcia-Castro M. Marcelle C. Bronner-Fraser M. Ectodermal Wnt function as a neural crest inducer. Science. 2002; 297: 848–851.

Gilbert, S. Developmental Biology 9th Edition. Sinauer Associates, Inc. Publishing. Sunderland (MA); 2010.

Hamburger V, Hamilton H L. A series of normal stages in the development of the chick embryo. Wiley-Liss, Inc. Hoboken (NJ); 1951.

Harper B, Beckerle M, Pomies P. Fine mapping of the alpha-actinin binding site within cysteine-rich protein. Biochemistry Journal. 2000; 350: 269-274.

Kalluir R, Weinberg R. The Basics of Epithelial-Mesenchyme Transition. The Journal of Clinical Investigation. 2009; 119(6): 1420-1428.

Khong T, Hague W. The Placenta in Maternal Hyperhomocysteinemia. Br J Obstet Gynaecol. 1999; 106: 273-278.

Kirby M. Cardiac Morphogenesis – Recent Research Advances. Pediatric Research. 1987; 21: 219-224.

Kirchner J, Forbush K, Bevan M. Identification and Characterization of Thymus LIM Protein: Targeted Disruption Reduces Thymus Cellularity. Molecular Cellular Biology. 2001; 21: 8592-8604.

Knight R, Schilling T. Cranial Neural Crest and Development of the Head Skeleton. Landes Bioscience; 2000.

Knoll R, Hoshijima M, Hoffman H, Person V, Lorenzen-Schmidt I, Bang M, Hayashi T, Shiga N, Yasukawa H, Schaper W, McKenna W, Yokoyama M et al. The Cardiac Mechanical Stretch Sensor Machinery Involves a Z Disc Complex that is Defective in a Subset of Human Dilated Cardiomyopathy. Cell. 2002; 111: 943-955.

Kong Y, Flick M, Kudla A, Konieczny S. Muscle LIM protein promotes myogenesis by enhancing the activity of MyoD. Molecular Cell Biology. 1997; 17: 4750-4760.

Konrat R, Weiskirchen R, Krautler B, Bister K. Solution structure of the carboxyl-terminal LIM domain from quail cysteine-rich protein CRP2. Journal of Biological Chemistry. 1997; 272: 12001-12007.

Kontaxis G, Konrat R, Krautler B, Weiskirchen R, Bister K. Structure and Intramodular Dynamics of the Amino-Terminal LIM Domain from Quail Cysteine- and Glycine-Rich Protein CRP2. Biochemistry. 1998; 37: 7127-7134.

Lai W, Kan M. Homocysteine-Induced Endothelial Dysfunction. Annuals of Nutrition & Metabolism. 2015; 67: 1-12.

Le Lievre, Le Douarin. Mesenchymal Derivatives of the Neural Crest: Analysis of Chimaeric Quail and Chick Embryos. Development. 1975; 34: 125-154.

Liu G, Zhang C, Wang G. Molecular Cloning, Characterization and Tissue Specificity of the Expression of the Ovine CSRP2 and CSRP3 Genes from Small-Tail Han Sheep (Ovis aries). Gene. 2016; 580(1): 47-57.

Loring J, Erickson C. Neural crest cell migratory pathways in the trunk of the chick embryo. Developmental Biology. 1987; 121(1): 220-236.

Louis H, Pino J, Schmeichel K, Pomies P, Beckerle M. Comparison of Three Members of the Cysteine-Rich Protein Family Reveals Functional Conservation and Divergent Patterns of Gene Expression. Journal of Biological Chemistry. 1997; 272: 27484-27491.

Mahmood L. The Metabolic Processes of Folic Acid and Vitamin B12 Deficiency. Journal of Health Research and Reviews. 2014; 1: 1-9.

Martins-Taylor K, Schroeder D, LaSalle J, Lalande M, Xu R. Role of DNMT3B in the Regulation of Early Neural and Neural Crest Specifiers. Epigenetics. 2012; 7(1): 71-82.

Megahed M, Taher I. Folate and Homocysteine Levels in Pregnancy. Continuing Education Topics & Issues. 2005; 290: 74-78.

Mica Y, Gabsang L, Stuart C, Tomishima M, Studer L. Modeling neural crest induction, melanocyte specification and disease-related pigmentation defects in hESCs and patient-specific iPSCs. Cell Rep. 2013; 3(4): 1140-1152.

Milinsky A, Jick H, Jick S. Multivitamin/folic acid supplementation in early pregnancy reduces the prevalence of neural tube defects. JAMA. 1989; 262**:** 2847-2852.

Minoux M, Rijli F. Molecular mechanisms of cranial neural crest cell migration and patterning in craniofacial development. Development. 2010; 137: 2605–2621.

Monie I, Nelson M. Abnormalities of pulmonary and other vessels in rat fetuses from maternal pteroylgutamic acid deficiency. Anat. Rec. 1963; 147: 397-405.

Nelson M, Asling C, Evans H. Production of multiple congenital abnormalities in young by maternal pteroylglutamic acid deficiency during gestation. J Nutr. 1952; 48:61–77.

Noden D M. Spatial integration among cells forming the cranial peripheral nervoud system. J. Neurobiology. 1993; 24: 248-261.

Panda D, Miao D, Lefebvre V, Hendy G, Goltzman D. The transcription factor SOX9 regulates cell cycle and differentiation genes in chondrocytic CFK2 cells. Journal of Biological Chemistry. 2001; 276: 41229–41236.

Prassler J, Murr A, Stocker S, Faix J, Murphy J, Marriott G. DdLIM is a Cytoskeleton-associated Protein Involved in the Protrusion of Lamellipodia in Dictyostelium. Molecular Biology Cell. 1998; 9(3): 545-559.

Rosenquist T. Folate, Homocysteine and the Cardiac Neural Crest. Developmental Dynamics. 2012; 242: 214-218.

Rosenquist T, Bennett G, Brauer P, Stewart M, Chaudoin T, Finnell R. Microarray Analysis of Homocystiene-Responsive Genes in Cardiac Neural Crest Cells In Vitro. Developmental Dynamics. 2007; 236:1044-1054.

Rosenquist T, Ratashak S, Selhum J. Homocysteine induces congenital defects of the heart and neural tube: Effect of folic acid. Proceedings of the National Academy of Sciences USA. 1996; 93: 15227-15232.

Sauka-Spengler T, Bronner-Fraser M. A gene regulatory network orchestrates neural crest formation. Nature Reviews Molecular Cell Biology. 2008; 9: 557-568.

Somaiah C, Kumar A, Mawrie D, Sharma A, Patil S, Bhattacharyya J, Swaminathan R, Jaganathan B. Collagen Promotes Higher Adhesion, Survival and Proliferation of Mesenchymal Stem Cells. PLOS ONE. 2015; 10(12): 1-15.

Stoya G, Klemm A, Baumann E, Vogelsang H, Ott U, Linuss W, Stein G. Determination of autofluorescence of red blood cells (RbCs) in uremic patients as a marker of oxidative damage. Clinical Nephrology. 2002; 58(3): 198-204.

Svoboda K, Hay E. Embryonic corneal epithelial interaction with exogenous laminin and basal lamina is F-actin dependent. Developmental Biology. 1987; 123(2): 455-469.

Vasiev B, Balter A, Chaplain M, Glazier J, Weijer C. Modeling gastrulation in the chick embryo: formation of the primitive streak. PLOS one. 2010; 5(5); e10571.

Waldo K, Miyagawa-Tomita S, Kumiski D, Kirby M. Cardiac Neural Crest Cells Provide New Insight into Septation of the Cardiac Outflow Tract: Aortic Sac to Ventricular Septal Closure. Developmental Biology. 1998; 196(2): 129-144.

Watkins D, Ru M, Hwang H, Kim C, Murray A, Philip N, Kim W, Legakis H, Wai T, Hilton J et al. Hyperhomocysteinemia Due to Methionone Synthase Deficincy, cblG: Structure of the MTRGene, Genotype Diversity, and Recognition of a Common Mutation, P1173L. American Journal of Human Genetics. 2002; 71: 143-153.

Zeng Z, Zhang H, Liu F, Zhang N. Current diagnosis and treatments for critical congenital heart defects. Experimental and Therapeutic Medicine. 2016; 11(5): 1550-1551